

First search for 2ε and $\varepsilon\beta^+$ decay of ^{174}Hf

F.A. Danevich^{a,1}, M. Hult^b, D.V. Kasperovych^a, G.P. Kovtun^{c,d}, K.V. Kovtun^e,
G. Lutter^b, G. Marissens^b, O.G. Polischuk^a, S.P. Stetsenko^c, V.I. Tretyak^a

^a*Institute for Nuclear Research, 03028 Kyiv, Ukraine*

^b*European Commission, Joint Research Centre, Retieseweg 111, 2440 Geel, Belgium*

^c*National Scientific Center “Kharkiv Institute of Physics and Technology”, 61108 Kharkiv,
Ukraine*

^d*Karazin Kharkiv National University, 61022 Kharkiv, Ukraine*

^e*Public Enterprise “Scientific and Technological Center Beryllium”, 61108 Kharkiv, Ukraine*

Abstract

The first ever search for 2ε and $\varepsilon\beta^+$ decay of ^{174}Hf was realized using a high-pure sample of hafnium (with mass 179.8 g) and the ultra low-background HPGe-detector system located 225 m underground. After 75 days of data taking no indication of the double beta decay transitions could be detected but lower limits for the half-lives of the different channels and modes of the decays were set on the level of $\lim T_{1/2} \sim 10^{16} - 10^{18}$ a.

Keywords: Double beta decay; ^{174}Hf , Low-background HPGe γ spectrometry

1 INTRODUCTION

A great interest to double beta (2β) decay, particularly to the neutrinoless mode of the process ($0\nu 2\beta$), is related to unique possibilities to clarify properties and nature of neutrino and weak interactions [1, 2, 3, 4, 5], and to test many other hypothetical scenarios of the $0\nu 2\beta$ decay [1, 3, 6, 7].

The efforts of experimentalists are concentrated mainly on the searches for the 0ν mode of 2β decay with electrons emission (see reviews [4, 8, 9, 10, 11, 12, 13, 14] and recent experimental works [15, 16, 17, 18, 19]). However, even the most sensitive experiments do not observe the effect and only set half-life limits on the level of $T_{1/2}^{0\nu 2\beta} > (10^{24} - 10^{26})$ a, that lead to the restrictions on the effective Majorana mass of electron neutrino on the level of (0.1 – 0.7) eV, depending on the nuclei and the nuclear matrix elements calculations. The sensitivity to the double beta plus processes: double electron capture (2ε), electron capture with positron emission ($\varepsilon\beta^+$), and double positron emission ($2\beta^+$) is much lower (we refer reader to the recent reviews [20, 21] and the references therein). At the same time, there is a strong motivation to improve sensitivities in studies of the double beta plus decay processes related to a possibility to clarify possible contribution of the right-handed currents to the $0\nu 2\beta$ decay rate in case of its observation [22].

¹Corresponding author. *E-mail address:* danevich@kinr.kiev.ua (F.A. Danevich).

The isotope ^{174}Hf is one of the potentially 2ε , $\varepsilon\beta^+$ radioactive nuclides with the energy of decay $Q_{2\beta} = 1100.0(23)$ keV [23] and the isotopic abundance $\delta = 0.16(12)\%$ [24]². A simplified expected decay scheme of ^{174}Hf is shown in Fig. 1. While the double electron capture is possible with population of the ground state and the first 2^+ excited level of the daughter nuclei, the electron capture with positron emission is allowed with the population of the ground state only (at least, for captures from K and L atomic shells, for which this process is the most probable). All the expected decays should be accompanied by single or multiple γ (X-ray) quanta emission that opens a possibility to apply HPGe γ spectrometry to search for the decays.

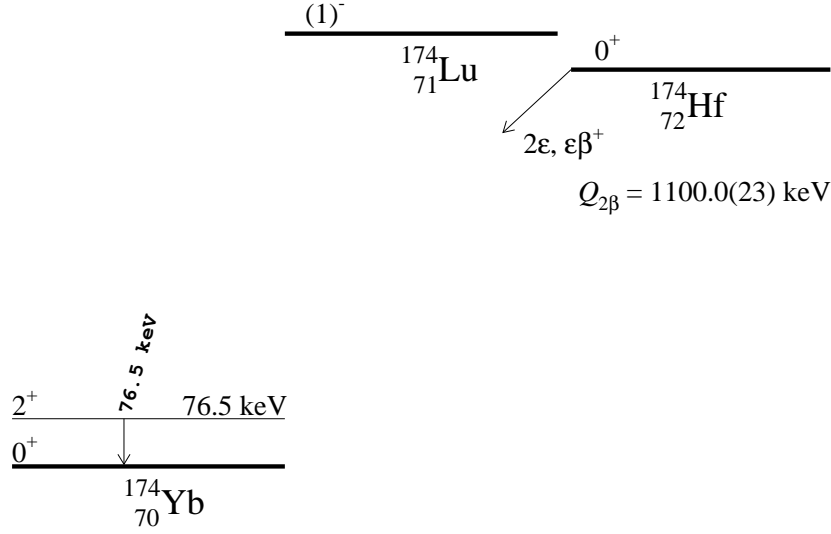


Figure 1: The simplified decay scheme of ^{174}Hf .

In Section 2 we describe the high-purity hafnium sample production and the experimental technique of ultra-low background HPGe γ spectrometry used in the present study. The data analysis and obtained limits on the 2ε and $\varepsilon\beta^+$ processes in ^{174}Hf are reported in Sect. 3. The Conclusions section contains a summary of the experiment and some discussion of possibilities to improve the experimental sensitivity.

2 Low counting experiment

2.1 Hafnium sample

A disc-shaped sample of metallic hafnium with sizes $\varnothing 59.0 \times 5.0$ mm (the mass of the sample was 179.8 g, the sample contained ≈ 0.29 g of the isotope ^{174}Hf) was utilized in the experiment. The hafnium was produced by the former Soviet Union industry by reduction process from hafnium tetrafluoride with metallic calcium. Then the material was purified by centrifugation of gaseous Hf compound to reduce zirconium concentration that is typically the main contaminant of hafnium, which is very hard to separate by chemical and physical methods. Finally the

²It should be stressed that so low isotopic abundance is typical for the potentially double beta plus active isotopes and is one of the practical reasons of the modest experimental sensitivity to this kind of nuclear instability.

material was additionally purified by double melting in vacuum by electron beam at the National Scientific Center “Kharkiv Institute of Physics and Technology” (Kharkiv, Ukraine). The purity level of the obtained hafnium was proved by the Laser Ablation Mass Spectrometry as $\simeq 99.8\%$ ³.

2.2 Gamma-ray spectrometry set-ups and measurements

The experiment was carried out with the help of two set-ups with three HPGe detectors (named Ge6, Ge7, and Ge10) at the HADES underground laboratory of the Joint Research Centre of European Commission (Geel, Belgium) located at 225 m depth below the ground. A schematic view of the both set-ups is presented in Fig. 2, while the main characteristics of the detectors are given in Table 1, with some more details in [25, 26, 27].

Table 1: Characteristics of the HPGe-detectors used in present experiment.

	Ge6	Ge7	Ge10
Energy resolution (FWHM) at 84 keV	1.4 keV	1.3 keV	0.9 keV
FWHM at 1332 keV	2.3 keV	2.2 keV	1.9 keV
Relative efficiency	80%	90%	62%
Ge crystal mass	2096 g	1778 g	1040 g
Window material and thickness	LB Cu 1.0 mm	HPAl 1.5 mm	HPAl 1.5 mm
Top dead layer thickness	0.9 mm	0.3 μm	0.3 μm

LB Cu = Low Background Copper

HPAl = High Purity Aluminum

The Hf sample was stored 13 days underground before the low background measurements to enable decay of short-lived cosmogenic radionuclides. In the first measurement the hafnium sample was installed directly on the endcap of the detector Ge10 (the “set-up I”, see Fig. 2). The measurements in the set-up were continued over 40.4 days with the Ge10 detector and 36.4 days with the detector Ge7. The Ge10 detector is developed for low-energy γ -rays measurements and has a very high energy resolution and high detection efficiency to γ quanta in the energy region $\approx (50 - 80)$ keV where most of the X-rays and γ quanta expected in the two-neutrino mode of the 2ε process to the ground state and to the lowest excited level 2^+ 76.5 keV of ^{174}Yb should be emitted. The Ge7 detector also has a rather high detection efficiency to low-energy γ quanta, despite a slightly worse energy resolution.

After the first stage, the experiment was continued for 34.8 days with the Ge6 detector instead of Ge10 (the second stage of the experiment is named “set-up II”). The Ge6 detector has a comparatively high detection efficiency to middle and high-energy γ quanta, however its sensitivity to low-energy γ quanta is substantially lower than that of the Ge7 and Ge10 detectors. Nevertheless, the detection efficiency of the detector Ge6 is high enough to detect γ quanta expected in the $0\nu 2\varepsilon$ and the $\varepsilon\beta^+$ processes with energies $\sim (0.5 - 1)$ MeV (see Section 3). Besides, the detector was useful to estimate radioactive contamination of the hafnium sample. The total exposure of the experiment was $42 \text{ g}\times\text{d}$ for the isotope ^{174}Hf ⁴.

³The purity level of the sample is reported in detail in our previous work aimed to the first search for α decays of naturally occurring Hf nuclides with emission of γ quanta [25].

⁴The exposure was calculated as a product of the isotope mass on the sum of measuring times of the four

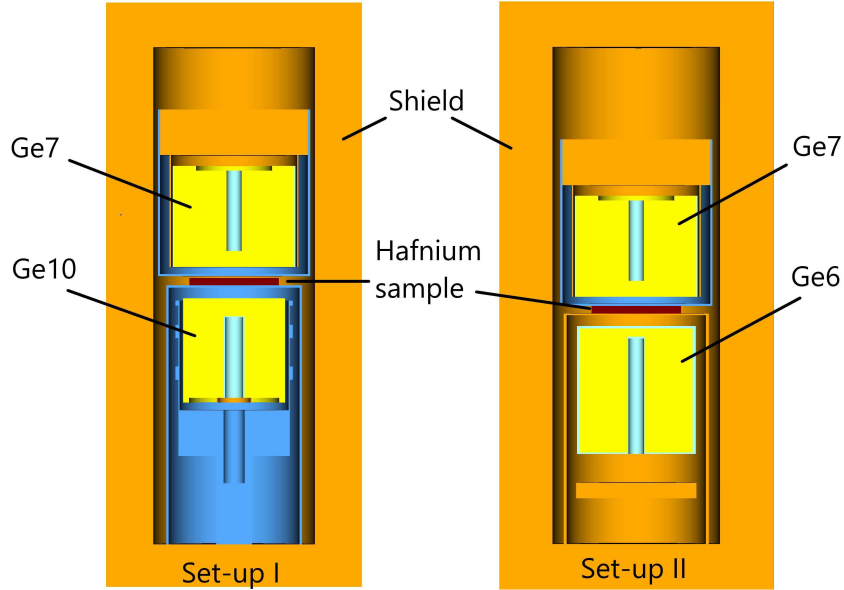


Figure 2: (Color online) Schematic view of the two low-background set-ups with HPGe detectors and hafnium sample.

Energy spectra measured in the set-up I by the HPGe detectors Ge7 and Ge10 are shown in Fig. 3, while the spectra accumulated in the set-up II are presented in Fig. 4. Background spectra, normalized on the time of measurements with the Hf sample, are shown in the Figures too.

There are many γ peaks in the data that can be ascribed to the naturally occurring primordial radionuclides: ^{40}K , daughters of the ^{232}Th , ^{235}U , and ^{238}U families. Some specific activities of hafnium radioactive nuclides were observed too: ^{175}Hf [electron capture with $Q_{EC} = 683.9(20)$ keV and the half-life $T_{1/2} = 70(2)$ days] and ^{181}Hf [beta active with $Q_{\beta} = 1035.5(18)$ keV, $T_{1/2} = 42.39(6)$ days]. It should be noted that the activities of the both radionuclides in the sample decrease in time due to decay in the underground conditions. We assume that the nuclides were generated by thermal neutron captures by ^{174}Hf and ^{180}Hf , respectively (both present in the Hf natural isotopic composition), and by interactions with high energy cosmic neutrons on the Earth surface, and especially, during the sample transportation by air.

Activities of the radionuclides in the hafnium sample were calculated with the following formula:

$$A = (S_{sample}/t_{sample} - S_{bg}/t_{bg})/(\xi \cdot \eta) \quad (1)$$

where S_{sample} (S_{bg}) is the area of a peak in the sample (background) spectrum; t_{sample} (t_{bg}) is the time of the sample (background) measurement; ξ is the γ -ray yield for the corresponding transition [28]; η is the full energy peak detection efficiency. The efficiencies were Monte Carlo simulated with the help of EGSnrc simulation package [29, 30]. The calculations were validated by comparison with the experimental data obtained with ^{109}Cd and ^{133}Ba γ sources (in the

detectors used in the experiment.

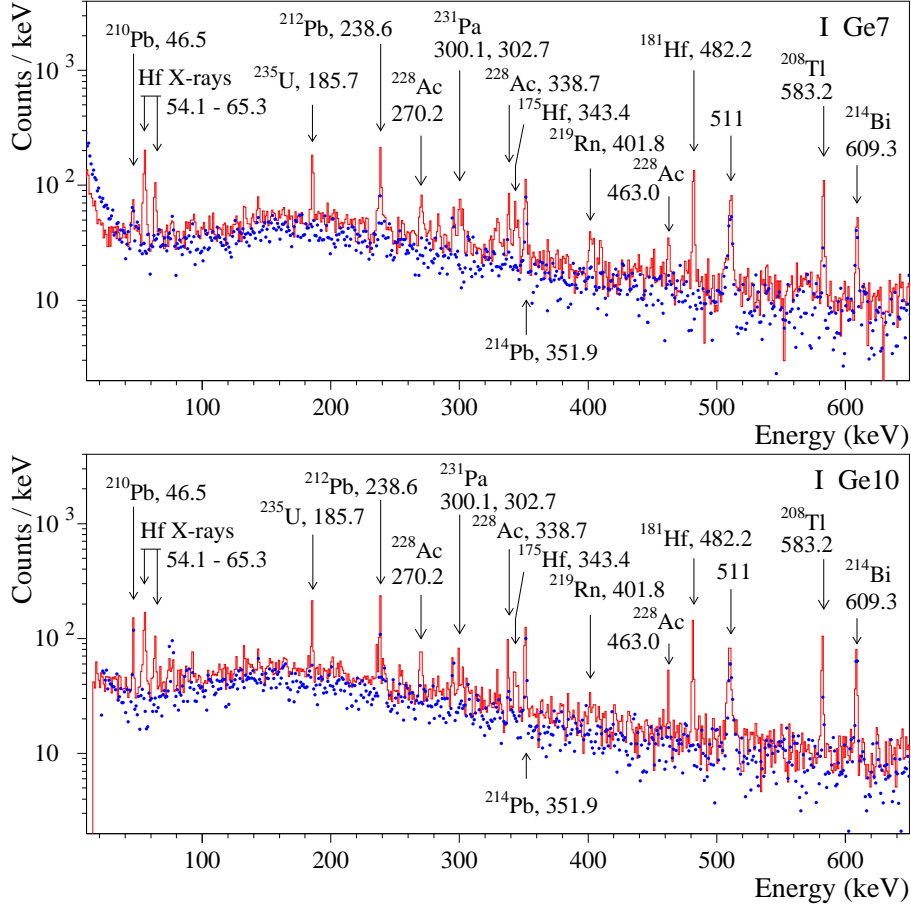


Figure 3: (Color online) Energy spectra accumulated with the Hf sample (solid line) and without sample (dots) by ultra-low-background HPGe γ detectors Ge7 (over 38.4 d with the hafnium sample and over 38.5 d without sample), and Ge10 (over 40.4 d with hafnium and 38.5 d background). The background energy spectra are normalized to the times of measurements with the Hf sample. Energy of γ and X-ray quanta are in keV.

set-up I), and ^{109}Cd , ^{133}Ba , ^{134}Cs , ^{152}Eu , ^{241}Am γ sources (set-up II). The standard deviation of the relative difference between the Monte Carlo simulations and the experiment is (5 – 7)% for γ peaks in the energy interval (53 – 384) keV for the set-up I, and is 6% for γ peaks in the energy interval (60 – 1408) keV for the set-up II. A summary of the estimated activities (limits) of radioactive impurities in the Hf sample is given in Table 2.

A peculiarity of the radioactive contamination is a significant deviation of the $^{235}\text{U}/^{238}\text{U}$ activities ratio in the Hf sample⁵. The excess of ^{235}U can be explained by the application of gas centrifugation method to remove zirconium in the hafnium production cycle (see Sec. 2). Despite the details of the production process are unknown, one could assume that the contamination by ^{235}U happened due to proximity between the industrial sites of the centrifugation facilities to purify hafnium and to enrich uranium. A more detailed discussion of the Hf sample radioactive contamination one can find in [25].

⁵The observed ratio is 0.36(18), while the expected one should be 0.046, assuming the natural isotopic abundance of the uranium isotopes.

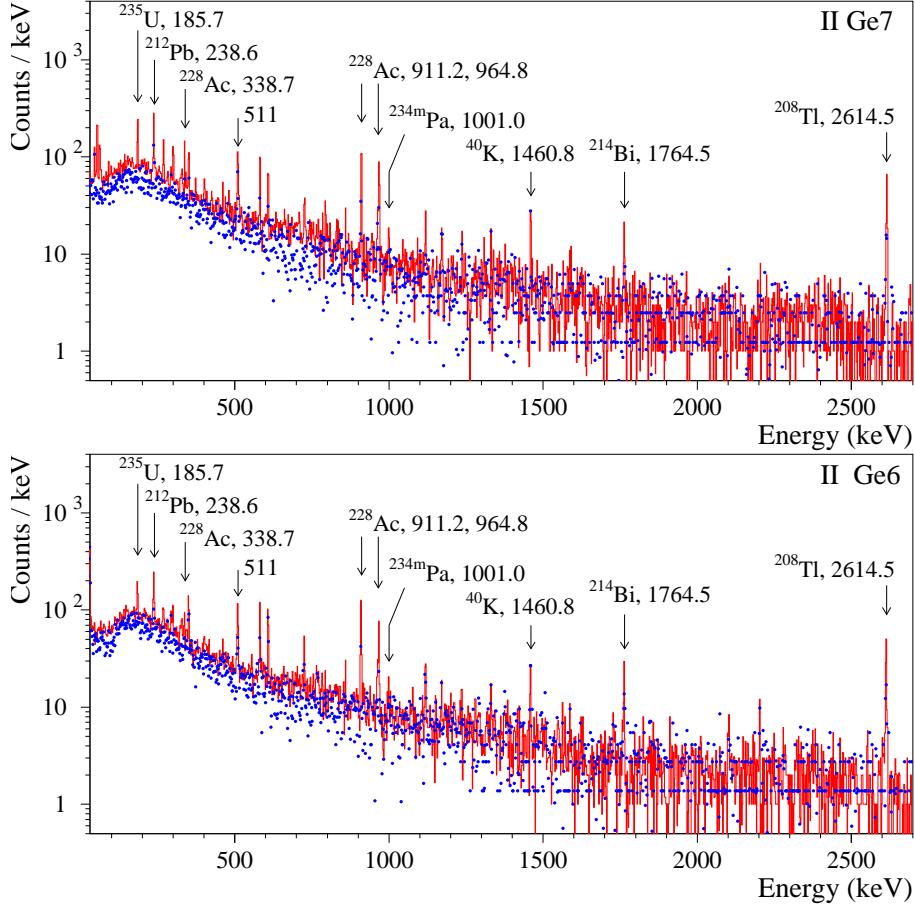


Figure 4: (Color online) Energy spectra accumulated with the hafnium sample (solid line) and without sample (dots) by ultra-low-background HPGe γ detectors Ge7 (over 34.8 d with the hafnium sample and over 28.1 d without sample), and Ge6 (over 34.8 d with hafnium and 25.3 d background). The background energy spectra are normalized to the times of measurements with the Hf sample. Energy of γ quanta are in keV.

3 Results and discussion

No peculiarity was observed in the experimental data that could be ascribed to the 2β decay processes in ^{174}Hf . Thus, we set limits on different modes and channels of the decay by using the following formula:

$$\lim T_{1/2} = N \cdot \eta \cdot t \cdot \ln 2 / \lim S, \quad (2)$$

where N is the number of ^{174}Hf nuclei in the sample (9.71×10^{20}), η is the detection efficiency for the effect searched for, t is the measuring time, and $\lim S$ is the number of events of the effect which can be excluded at a given confidence level (C.L.). The detection efficiencies of the detectors to the γ (X-ray) quanta expected in different modes and channels of the double beta processes in ^{174}Hf were simulated with the EGSnrc simulation package [29, 30], the decay events were generated by the DECAY0 events generator [31].

Table 2: Radioactive contamination of the Hf sample measured by HPGe γ -ray spectrometry. The activities of ^{175}Hf and ^{181}Hf are given with reference date at the start of each measurement for Set-up I and Set-up II (within brackets) separately. Upper limits are given at 90% C.L., the reported uncertainties are the combined standard uncertainties.

Chain	Nuclide	Activity in the sample (mBq)
	^{40}K	≤ 1.4
	^{60}Co	≤ 0.11
	^{137}Cs	≤ 0.20
	^{172}Hf	≤ 3
	^{175}Hf	0.44 ± 0.05 (0.18 ± 0.04)
	$^{178m2}\text{Hf}$	≤ 0.06
	^{181}Hf	1.45 ± 0.07 (0.12 ± 0.04)
	^{182}Hf	≤ 0.5
^{232}Th	^{228}Ra	3.6 ± 0.7
	^{228}Th	2.38 ± 0.25
^{235}U	^{235}U	3.8 ± 0.5
	^{231}Pa	11 ± 3
	^{227}Ac	2.0 ± 0.5
^{238}U	^{234m}Pa	11 ± 5
	^{226}Ra	≤ 0.7
	^{210}Pb	≤ 50

3.1 Search for double electron capture processes in ^{174}Hf

In case of the $2K$ and KL capture in ^{174}Hf , a cascade of X-rays (and Auger electrons) of Yb atom with individual energies, in particular, in the energy interval (50.8 – 61.3) keV is expected, while energies of the $2L$ capture X-ray quanta are $\approx (7 - 10)$ keV, that are below the detectors' energy thresholds. We took into account only the most intense X-rays of ytterbium [28]: 51.4 keV (the intensity of the X-ray quanta is 27.2%), 52.4 keV (47.4%), 59.2 keV (5.2%), 59.4 keV (10.0%), and 61.0 keV (3.4%). The energy spectra accumulated with the Hf sample were fitted by the sum of several Gaussian functions: five peaks of $2\nu 2K$ decay of ^{174}Hf with energies (51.4 – 61.0) keV, a peak of ^{210}Pb with energy 46.5 keV, Gaussian functions to describe the X-ray peaks of Hf, the 63.3 keV peak of ^{234}Th , 67.7 keV peak of ^{230}Th and a straight line to describe the continuous background. A highest sensitivity to the effect was achieved by analysis of a sum spectrum of the detectors Ge7, Ge10 in the set-up I and of the Ge7 detector in the set-up II. The individual energy dependencies of the detectors energy resolutions were taken into account in the model. The data of the Ge6 detector was not used taking into account a rather low detection efficiency of the detector to low-energy γ (X-ray) quanta. The best fit was achieved in the energy interval (39 – 71) keV⁶ with $\chi^2/\text{n.d.f.} = 41.6/47 = 0.89$, where n.d.f. is number of degrees of freedom. The fit gives an area of the effect -7 ± 26 counts. By using

⁶It should be noted that also two X-ray quanta with a total energy up to ≈ 122 keV could be detected in coincidence in the $2\nu 2K$ process, however, the detection efficiency to the events is substantially lower than that to one K X-ray quanta.

the recommendations [32], we took 36 counts as $\text{lim } S$ with 90% confidence level (C.L.)⁷. The sum energy spectrum in the vicinity of the effect and the model of background are presented in Fig. 5 together with the excluded effect. It should be noted that here and below the estimations of the $\text{lim } S$ values include only the statistical errors coming from the data fluctuations, and that systematic contributions have not been considered. However, the statistical errors already do include correlations to the background model. The detection efficiency for the effect was calculated by the following formula:

$$\eta = \sum \eta_i \times t_i / \sum t_i, \quad (3)$$

where η_i are the individual detection efficiencies and t_i are the measuring times of the detectors used in the analysis. The detection efficiency is estimated to be 1.24% for the whole X-rays distribution, and the following limit on the $2\nu 2K$ decay of ^{174}Hf to the ground state of ^{174}Yb was set: $T_{1/2}^{2\nu 2K} \geq 7.1 \times 10^{16}$ a. The detection efficiency to the X-ray quanta in the energy interval (51.4 – 61.0) keV in the case of the $2\nu KL$ decay in ^{174}Hf to the ground state of ^{174}Yb is lower (0.73%) that results in the following half-life limit: $T_{1/2}^{2\nu KL} \geq 4.2 \times 10^{16}$ a. The results are presented in Table 3 together with the values of the $\text{lim } S$ and the detection efficiencies.

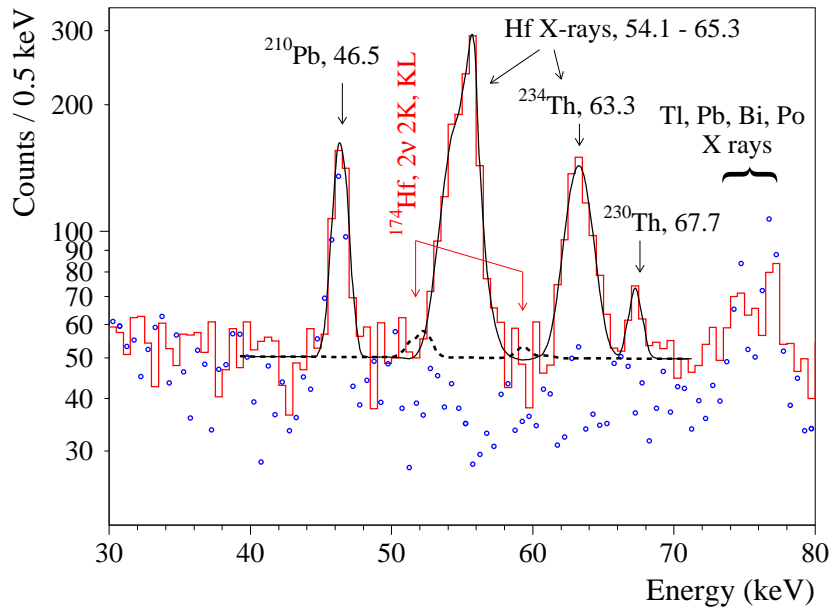


Figure 5: (Color online) The sum energy spectrum collected with the detectors Ge7, Ge10 in the set-up I, plus the Ge7 detector in the set-up II (solid histogram) in the energy region where K X-ray quanta are expected for the $2\nu 2K$ and $2\nu KL$ decays of ^{174}Hf . The fit of the data by the background model is shown by solid line, while the excluded effect is presented by dashed line. The background data accumulated with the detectors, normalized on the measuring time, are shown by dots. Energy of γ and X-ray quanta are in keV.

⁷All the limits in the present work were set with 90% C.L. by using the recommendations [32].

Table 3: The half-life limits on 2ε and $\varepsilon\beta^+$ processes in ^{174}Hf . The energies of the γ quanta (E_γ), which were used to set the $T_{1/2}$ limits, are listed with their corresponding detection efficiencies (η) and values of $\lim S$.

Channel of decay	Decay mode	Level of daughter nucleus (keV)	E_γ (keV)	η (%)	$\lim S$ (counts) at 90% C.L.	Experimental limit $T_{1/2}$ (a) at 90% C.L.
$2K$	2ν	g.s.	51.4 – 61.0	1.24	36	$\geq 7.1 \times 10^{16}$
KL	2ν	g.s.	51.4 – 61.0	0.73	36	$\geq 4.2 \times 10^{16}$
$2K$	2ν	2^+ 76.5	51.4 – 61.0	1.03	36	$\geq 5.9 \times 10^{16}$
KL	2ν	2^+ 76.5	51.4 – 61.0	0.61	36	$\geq 3.5 \times 10^{16}$
$2L$	2ν	2^+ 76.5	76.5	0.39	20.4	$\geq 3.9 \times 10^{16}$
$2K$	0ν	g.s.	977.4	4.53	10.0	$\geq 5.8 \times 10^{17}$
KL	0ν	g.s.	1028.9	4.46	3.0	$\geq 1.9 \times 10^{18}$
$2L$	0ν	g.s.	1080.4	4.39	7.2	$\geq 7.8 \times 10^{17}$
$2K$	0ν	2^+ 76.5	900.9	4.67	8.4	$\geq 7.1 \times 10^{17}$
KL	0ν	2^+ 76.5	952.4	4.59	9.5	$\geq 6.2 \times 10^{17}$
$2L$	0ν	0^+ 76.5	1003.9	4.51	8.0	$\geq 7.2 \times 10^{17}$
$K\beta^+$	$(2\nu+0\nu)$	g.s.	511	10.6	202	$\geq 1.4 \times 10^{17}$
$L\beta^+$	$(2\nu+0\nu)$	g.s.	511	10.7	202	$\geq 1.4 \times 10^{17}$

A similar group of Yb K X-ray quanta is expected also in the $2\nu 2K$ and $2\nu KL$ decays of ^{174}Hf to the first 2^+ 76.5 keV excited level of ^{174}Yb . The sensitivity with the (51.4 – 61.0) keV X-ray quanta analysis is higher than that with the 76.5 keV γ quanta. The reasons are: 1) a higher detection efficiency to the X-ray quanta (in particular, because in deexcitation of the 76.5 keV level mostly electrons are emitted, conversion coefficient is equal 9.43 [33], while the set-up is not sensitive to these electrons); 2) a rather high counting rate in the vicinity of the energy 76.5 keV due to the background caused by X-rays of Tl, Pb, Bi and Po. Thus, the limits on the $2\nu 2K$ and $2\nu KL$ decays to the 76.5 keV level were derived from the analysis of the energy region where the group of (51.4 – 61.0) keV X-ray quanta is expected (see Fig. 5). The detection efficiencies, excluded effects' areas and obtained half-life limits are presented in Table 3.

However, the limit for $2\nu 2L$ process was obtained by analysis of the 76.5 keV peak in the experimental data, taking into account that L X-ray quanta are below the acquisition energy threshold of our experimental set-ups and cannot be detected in the present experiment. The analysis of the data near 76.5 keV is rather complicated, since there are many X-ray peaks in the energy region. Thus, we have fitted the experimental sum spectrum of the three detectors in the energy interval around the energy 76.5 keV by sum of the most intensive K X-ray quanta of Tl (72.9 keV), Pb (75.0 keV), Bi (77.1 keV and 87.3 keV), Po (76.9 keV, 79.3 keV) and Rn (81.1 keV, 83.8 keV). The model describes the experimental data rather well with the $\chi^2/\text{n.d.f.} = 41.6/47 = 0.72$, giving the 76.5 keV peak area $S = 5.0 \pm 9.4$ counts, that corresponds to $\lim S = 20.4$ counts. The sum energy spectrum of the detectors Ge7, Ge10 (set-up I) and of the detector Ge7 (set-up II) in the energy region 50 – 100 keV is presented in Fig. 6 together with the background model and the excluded peak with energy 76.5 keV.

The obtained half-life limit on the $2\nu 2L$ decay of ^{174}Hf to the first 2^+ 76.5 keV excited level of ^{174}Yb is given in Table 3.

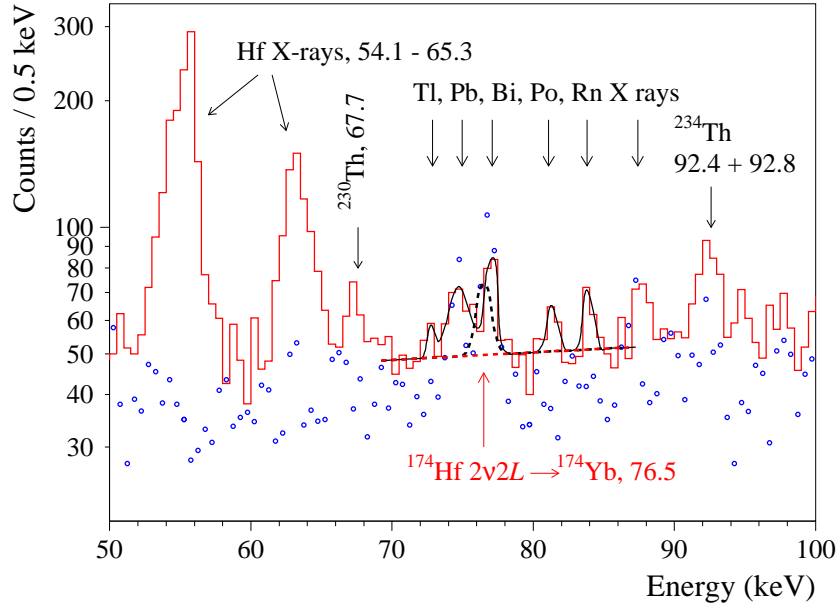


Figure 6: (Color online) Part of the sum energy spectrum collected with the detectors Ge7, Ge10 in the set-up I, and with the Ge7 detector in the set-up II (solid histogram) in the energy region where 76.5 keV γ quanta emitted in the $2\nu 2L$ decay of ^{174}Hf to the first 2^+ 76.5 keV excited level of ^{174}Yb are expected together with the model of background (solid line). The excluded 76.5 keV peak with area 20.4 counts is shown by dashed line. The background energy spectrum accumulated with the detectors, normalized on the measuring time, is shown by dots. Energy of γ and X-ray quanta are in keV.

In case of the 0ν double electron capture in ^{174}Hf from K and L shells to the ground state of the daughter nuclei, we suppose that the energy excess in the process is taken away by bremsstrahlung γ quanta with an energy: $E_\gamma = Q_{2\beta} - E_{b1} - E_{b2}$, where E_{bi} are the binding energies of the captured electrons on the K and L atomic shells of the daughter Yb nuclide. The energy spectrum measured with the Hf sample by the detectors Ge7 and Ge6 in the set-up II⁸ was fitted by a model constructed from a peak searched for and a 1st degree polynomial function to describe the continuous background (see Fig. 7). In the case of the $0\nu 2L$ decay, the γ peak of ^{212}Bi with energy 1078.8 keV was also included in the background model. The energy of the Gaussian function used to describe the effect was varied taking into account the uncertainty of the $Q_{2\beta}$ value (± 2.3 keV). The fits to the energy spectrum provided (5.4 ± 2.8) counts, (-1.5 ± 2.2) counts, and (3.3 ± 2.4) counts for the $0\nu 2K$, $0\nu KL$, and $0\nu 2L$ peaks, respectively. The corresponding $\lim S$ values are 10.0, 3.0 and 7.2 counts. The excluded peaks are also shown in Fig. 7.

⁸The data gathered in the set-up I were not used in the analysis due to the restricted at ~ 0.7 MeV upper energy thresholds of the detectors. The amplification was increased with the intention to enable better peak-definitions in the low-energy region of the spectrum by having more channels per peak.

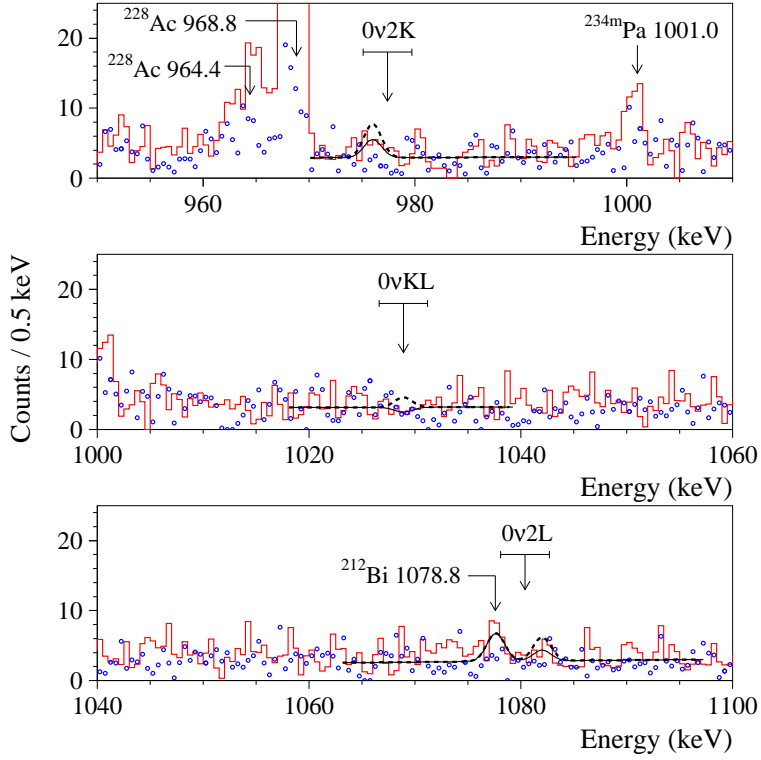


Figure 7: (Color online) Parts of the sum energy spectrum accumulated with the Hf sample by the detectors Ge7 and Ge6 in the set-up II, where the γ peaks from the $0\nu 2K$ (upper panel), $0\nu KL$ (middle panel), and $0\nu 2L$ (lower panel) captures in ^{174}Hf to the ground state of ^{174}Yb are expected. The fit of the data are shown by solid lines, while the excluded peaks are presented by dashed lines. The horizontal lines (above the arrows labelling the energy of the peaks searched for) show the energy interval ± 2.3 keV corresponding to the uncertainty of the $Q_{2\beta}$ value of ^{174}Hf . The background data accumulated with the detectors, normalized on the measuring time, are shown by dots. The energy of the background γ peaks are in keV.

A similar analysis was performed also for the 0ν double electron capture transitions to the 2^+ 76.5 keV excited level of ^{174}Yb . The results of the analysis are shown in Fig. 8. The obtained lower half-life limits for the $0\nu 2\varepsilon$ decays of ^{174}Hf to the ground and the 2^+ 76.5 keV excited level of ^{174}Yb are given in Table 3.

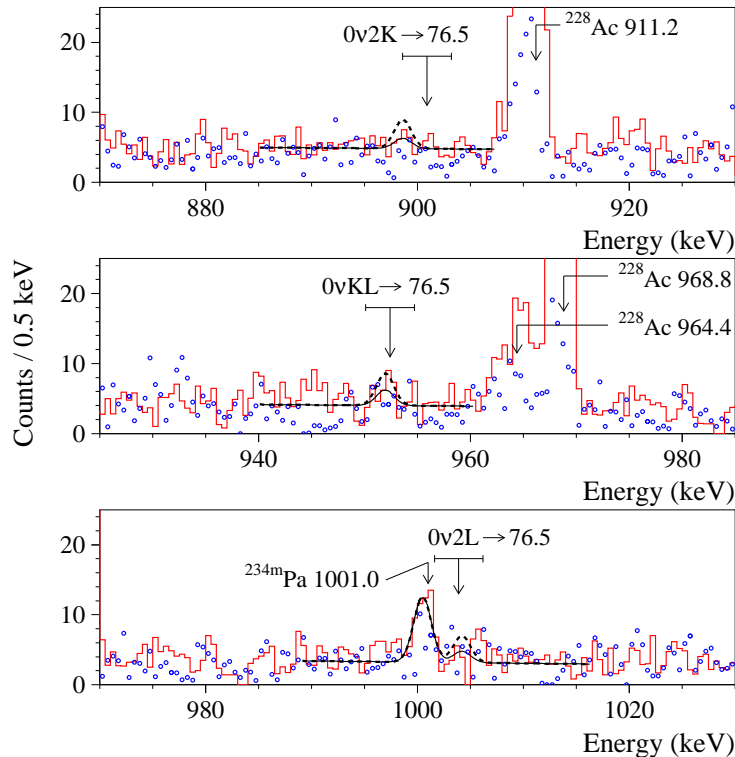


Figure 8: (Color online) Parts of the sum energy spectrum accumulated with the Hf sample by the Ge7 and Ge6 detectors in the set-up II, where the γ peaks from the $0\nu 2K$ (upper panel), $0\nu KL$ (middle panel), and $0\nu 2L$ (lower panel) captures in ^{174}Hf to the 2^+ 76.5 keV excited level of ^{174}Yb are expected. The fits of the data are shown by solid lines, while the excluded peaks are presented by dashed lines. The horizontal lines (above the arrows labelling the energy of the peaks searched for) show the energy interval ± 2.3 keV corresponding to the uncertainty of the $Q_{2\beta}$ value of ^{174}Hf . The background data accumulated with the detectors, normalized on the measuring time, are shown by dots. The energy of the background γ quanta are in keV.

3.2 Search for electron capture with positron emission in ^{174}Hf

One positron with an energy up to 78 ± 2.3 keV should be emitted in the $\varepsilon\beta^+$ decay of ^{174}Hf . The annihilation of the positron should give two 511 keV γ 's leading to an extra counting rate in the annihilation peak. The sum of all four detectors' energy spectra was fitted in the energy interval (495 – 530) keV with a simple model constructed from a 511 keV peak (with a free parameter that describe the peak's width) and a 1st degree polynomial function to describe background. The fits of the experimental data in the vicinity of the annihilation peak are shown in Fig. 9. There are 783 ± 33 counts in the peak in the data accumulated with the hafnium sample, and 508 ± 32 counts in the background data. The Monte Carlo simulations show that

the main part of the excess (153 ± 17 counts) can be explained by decays of ^{228}Ac and ^{208}Tl in the Hf sample. The residual peak area of 122 ± 49 counts, despite showing excess of more than two sigma, cannot be accepted as effect of electron capture with positron emission in ^{174}Hf . The difference indicates presence of some systematics, that needs more careful investigations, e.g., by using isotopically enriched sample. Thus, assuming that the 511 keV peak excess provides no evidence of the effect searched for, 202 counts should be accepted as $\text{lim } S$. Taking into account the detection efficiency 10.6% (10.7%) for $K\beta^+$ ($L\beta^+$) decay mode, we have obtained the same limit on the half-life of ^{174}Hf relatively to the electron capture from the K and L shells of daughter atom with positron emission in ^{174}Hf : $T_{1/2} \geq 1.4 \times 10^{17}$ a. The limits are presented in Table 3. The limits are valid for both the 2ν and 0ν modes of the decay, since the modes cannot be distinguished by the γ spectrometry method.

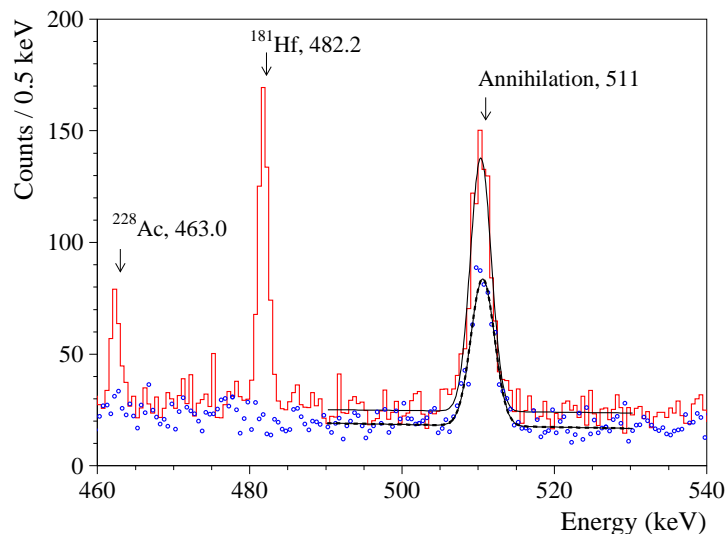


Figure 9: (Color online) Part of the energy spectra measured with the Hf sample by the detectors Ge7, Ge10 (set-up I) and Ge7, Ge6 (set-up II) in the vicinity of the 511 keV annihilation peak. The background data accumulated with the detectors, normalized on the measuring time with the Hf sample, are shown by dots. The fits of the data are shown by solid lines. The energy of the background γ peaks are in keV.

4 Conclusions

A highly purified hafnium-disc with mass 179.8 g and the dimensions $\varnothing 59.0 \times 5.0$ mm was obtained by using the double melting in vacuum by electron beam of a high purity sample of metallic hafnium. The material was measured in the HPGe-detector γ -ray spectrometry system located 225 m underground at the HADES laboratory with an aim to search (at the first time) for 2ε and $\varepsilon\beta^+$ decay of ^{174}Hf . No effect was observed after 75 days of data taking but lower limits on the half-lives for the different channels and modes of the decays were set on the level of $\text{lim } T_{1/2} \sim 10^{16} - 10^{18}$ a.

The sensitivity of the experiment could be advanced by using even more highly purified from trace radioactive impurities hafnium enriched in the isotope ^{174}Hf , increasing the exposure,

and detection efficiency by application of thinner samples and multi-crystal system of HPGe detectors. It should be stressed that such an experiment looks practically realizable thanks to a general possibility to apply gas centrifugation for Hf isotopical enrichment, for the moment only the viable technology to produce large enough amount of isotopically enriched materials.

5 Acknowledgments

This project received support from the EC-JRC open access project EUFRAT under Horizon 2020. The group from the Institute for Nuclear Research (Kyiv, Ukraine) was supported in part by the program of the National Academy of Sciences of Ukraine “Fundamental research on high-energy physics and nuclear physics (international cooperation)”. D.V.K. and O.G.P. were supported in part by the project “Investigations of rare nuclear processes” of the program of the National Academy of Sciences of Ukraine “Laboratory of young scientists” (Grant No. 0118U002328).

References

- [1] M.J. Dolinski, A.W.P. Poon, W. Rodejohann, Neutrinoless Double-Beta Decay: Status and Prospects, *Annu. Rev. Nucl. Part. Sci.* 69 (2019) 219.
- [2] J. Barea, J. Kotila, F. Iachello, Limits on Neutrino Masses from Neutrinoless Double- β Decay, *Phys. Rev. Lett.* 109 (2012) 042501.
- [3] W. Rodejohann, Neutrino-less double β decay and particle physics, *J. Phys. G* 39 (2012) 124008.
- [4] S. Dell’Oro, S. Marcocci, M. Viel, F. Vissani, Neutrinoless Double Beta Decay: 2015 Review, *AHEP 2016* (2016) 2162659.
- [5] J.D. Vergados, H. Ejiri, F. Simkovic, Neutrinoless double beta decay and neutrino mass, *Int. J. Mod. Phys. E* 25 (2016) 1630007.
- [6] F.F. Deppisch, M. Hirsch, H. Päs, Neutrinoless double- β decay and physics beyond the standard model, *J. Phys. G* 39 (2012) 124007.
- [7] S.M. Bilenky, C. Giunti, Neutrinoless double- β decay: A probe of physics beyond the standard model, *Int. J. Mod. Phys. A* 30 (2015) 1530001.
- [8] V.I. Tretyak, Yu.G. Zdesenko, Tables of double β decay data – an update, *At. Data Nucl. Data Tables* 80 (2002) 83.
- [9] S.R. Elliott, Recent progress in double beta decay, *Mod. Phys. Lett. A* 27 (2012) 123009.
- [10] A. Giuliani, A. Poves, Neutrinoless Double-Beta Decay, *AHEP 2012* (2012) 857016.
- [11] R. Saakyan, Two-Neutrino Double-Beta Decay, *Annu. Rev. Nucl. Part. Sci.* 63 (2013) 503.
- [12] O. Cremonesi, M. Pavan, Challenges in Double Beta Decay, *AHEP 2014* (2014) 951432.

- [13] J.J. Gómez-Cadenas, J. Martín-Albo, Phenomenology of Neutrinoless Double Beta Decay, Proc. of Sci. (GSSI14) 004 (2015).
- [14] X. Sarazin, Review of Double Beta Experiments, J. Phys.: Conf. Ser. 593 (2015) 012006.
- [15] M. Agostini et al., Probing Majorana neutrinos with double- β decay, Science 365 (2019) 1445.
- [16] G. Anton et al. (The EXO-200 Collaboration), Search for Neutrinoless Double-Beta Decay with the Complete EXO-200 Dataset, Phys. Rev. Lett. 123 (2019) 161802.
- [17] C. Alduino et al. (CUORE Collaboration), First Results from CUORE: A Search for Lepton Number Violation via $0\nu\beta\beta$ Decay of ^{130}Te , Phys. Rev. Lett. 120 (2018) 132501.
- [18] R. Arnold et al., Results of the search for neutrinoless double- β decay in ^{100}Mo with the NEMO-3 experiment, Phys. Rev. D 92 (2015) 072011.
- [19] A. Gando et al. (KamLAND-Zen Collaboration), Search for Majorana Neutrinos Near the Inverted Mass Hierarchy Region with KamLAND-Zen, Phys. Rev. Lett. 117 (2016) 082503.
- [20] J. Maalampi, J. Suhonen, Neutrinoless Double β^+ /EC Decays, AHEP 2013 (2013) 505874.
- [21] K. Blaum et al., Double-Electron Capture, in preparation.
- [22] M. Hirsch, K. Muto, T. Oda, H.V. Klapdor-Kleingrothaus, Nuclear structure calculation of $\beta^+\beta^+$, β^+ /EC and EC/EC decay matrix elements, Z. Phys. A 347 (1994) 151.
- [23] M. Wang et al., The AME2016 atomic mass evaluation, (II). Tables, graphs and references, Chin. Phys. C 41 (2017) 030003.
- [24] J. Meija et al., Isotopic compositions of the elements 2013 (IUPAC Technical Report), Pure Appl. Chem. 88 (2016) 293.
- [25] F.A. Danevich et al., First search for α decays of naturally occurring Hf nuclides with emission of γ quanta, arXiv:1910.02262v1 [nucl-ex], accepted to Eur. Phys. J. A.
- [26] J.S.E. Wieslander et al., The Sandwich spectrometer for ultra low-level γ -ray spectrometry, Appl. Radiat. Isot. 67 (2009) 731.
- [27] M. Hult et al., Comparison of background in underground HPGe-detectors in different lead shield configurations, Appl. Radiat. Isot. 81 (2013) 103.
- [28] R.B. Firestone et al., *Table of Isotopes*, 8th ed. (John Wiley, N.Y., 1996) and CD update (1998).
- [29] I. Kawrakow et al., The EGSnrc Code System: Monte Carlo simulation of electron and photon transport. Technical Report PIRS-701, National Research Council Canada (2017).
- [30] G. Lutter, M. Hult, G. Marissens, H. Stroh, F. Tzika, A gamma-ray spectrometry analysis software environment, Appl. Radiat. Isot. 134 (2018) 200.

- [31] O.A. Ponkratenko et al., Event Generator DECAY4 for Simulating Double-Beta Processes and Decays of Radioactive Nuclei, *Phys. At. Nucl.* 63 (2000) 1282.
- [32] G.J. Feldman, R.D. Cousins, Unified approach to the classical statistical analysis of small signals, *Phys. Rev. D* 57 (1998) 3873.
- [33] E. Browne, H. Junde, Nuclear Data Sheets for $A = 174$, *Nucl. Data Sheets* 87 (1999) 15.